



Structural and optical characterization of single-phase γ - In_2Se_3 films with room-temperature photoluminescence

D.Y. Lyu^a, T.Y. Lin^{a,*}, T.W. Chang^a, S.M. Lan^b, T.N. Yang^c, C.C. Chiang^c, C.L. Chen^a, H.P. Chiang^{a,d}

^a Institute of Optoelectronic Sciences, National Taiwan Ocean University, No. 2, Beining Rd., Keelung 20224, Taiwan

^b Department of Electronic Engineering, Chung Yuan Christian University, Chung-Li 32023, Taiwan

^c Institute of Nuclear Energy Research (INER), Atomic Energy Council, Taoyuan County 32546, Taiwan

^d Institute of Physics, Academia Sinica, Taipei 11529, Taiwan

ARTICLE INFO

Article history:

Received 2 February 2010

Received in revised form 11 March 2010

Accepted 13 March 2010

Available online 19 March 2010

PACS:

81.05.Hd

81.15.Gh

78.55.Hx

Keywords:

InSe

MOCVD

Photoluminescence

ABSTRACT

The single-phase γ - In_2Se_3 films with red room-temperature photoluminescence (PL) have been realized by atmospheric metal-organic chemical vapor deposition at the temperature range of 350–500 °C. The crystal structure of the γ - In_2Se_3 films was determined by X-ray diffraction and Raman spectroscopy. From the temperature dependence of the free exciton line, the room-temperature energy gap of γ - In_2Se_3 films is found to be about 1.947 eV. At 10 K, the free exciton emissions was observed and located at 2.145 eV. The temperature dependence of the near band-edge emission in the temperature region of 10–300 K has been investigated. The measured peak energy of near band-edge emission redshifts by about 200 meV with increasing temperature from 10 to 300 K, and is expressed by, $E_g(T) = 2.149 + ((-8.50 \times 10^{-4})T^2 / (T + 75.5))$ eV. This study was done to complete the reported information about γ - In_2Se_3 thin films.

© 2010 Elsevier B.V. All rights reserved.

1. Introduction

The In_2Se_3 (IS) compound semiconductors have several different crystalline phase, i.e., layered structure (α -phase) [1], rhombohedral structure (β -phase) [2,3], defect wurtzite structure (γ -phase) [4] and anisotropic structure (κ -phase) [5]. Recently, γ - In_2Se_3 is found to be a promising candidate that can be used for Cd-free buffer layer for CIGS solar cell [6]. The In_2Se_3 films have been grown by sputtering [7], annealing of cold-deposited In/Se multilayers [8], molecular beam epitaxy [4,9,10], etc. in early research. Metal-organic chemical vapor deposition (MOCVD) has many advantages in material growth such as high crystalline quality, growth rate, large area uniformity and volume production. Using MOCVD to deposit In_2Se_3 is worth exploring for the growth of In_2Se_3 .

In_2Se_3 thin film has been grown by single source MOCVD, which composition ratio of the Se/In cannot be varied [11,12]. Recently, In_2Se_3 films have been grown with dual source precursors to vary the VI/III ratio and to get the best parameters for crystal quality. For example, there are a few reports on the growth of γ - In_2Se_3

films on Si(1 1 1) or Si(1 0 0) substrates by MOCVD using H_2Se and TMI precursors [13–15]. However, the as-grown γ - In_2Se_3 epitaxial thin films can emit photoluminescence (PL) only at low temperature, which limit a complete understanding of their properties. It insinuates that we can reform the quality of γ - In_2Se_3 films further. The low-temperature (LT) buffer layers are usually used to reduce heterointerface strain in heteroepitaxy. LT In_xSe_y buffer layer could possibly relax lattice misfit because it crystallizes between γ - In_2Se_3 films and substrates. In this study, we deposited the γ - In_2Se_3 films with red room-temperature (RT) PL using LT In_xSe_y buffer layer on Si(1 1 1) substrate.

2. Experimental details

Five samples named as IS350, IS375, IS400, IS450 and IS500 were studied here. The deposition temperatures for IS350, IS375, IS400, IS450 and IS500 samples were 350, 375, 400, 450 and 500 °C, respectively. The samples were grown on Si(1 1 1) substrate with LT In_xSe_y buffer layer by atmospheric MOCVD. Metal-organic precursors used were H_2Se for Se and TMI for In. Si(1 1 1) substrates were cleaned by standard RCA clean process. After loaded into reactor, Si substrate was thermally cleaned to remove native oxide at 1100 °C for 10 min in hydrogen ambient. The substrate was then cooled down for the In_2Se_3 growth. LT In_xSe_y buffer layer was first deposited at 200 °C for 10 min. Then, high-temperature γ - In_2Se_3 thin films were grown at 350, 375, 400, 450 and 500 °C for 35 min, respectively.

The surface morphology of the γ - In_2Se_3 thin films was explored by scanning electron microscopy (SEM). The structural and phase properties of γ - In_2Se_3 thin films were investigated by X-ray diffraction (XRD) and Raman spectroscopy.

* Corresponding author. Tel.: +886 2 2462 2192x6703; fax: +886 2 2462 0724.

E-mail address: tylin@mail.ntou.edu.tw (T.Y. Lin).

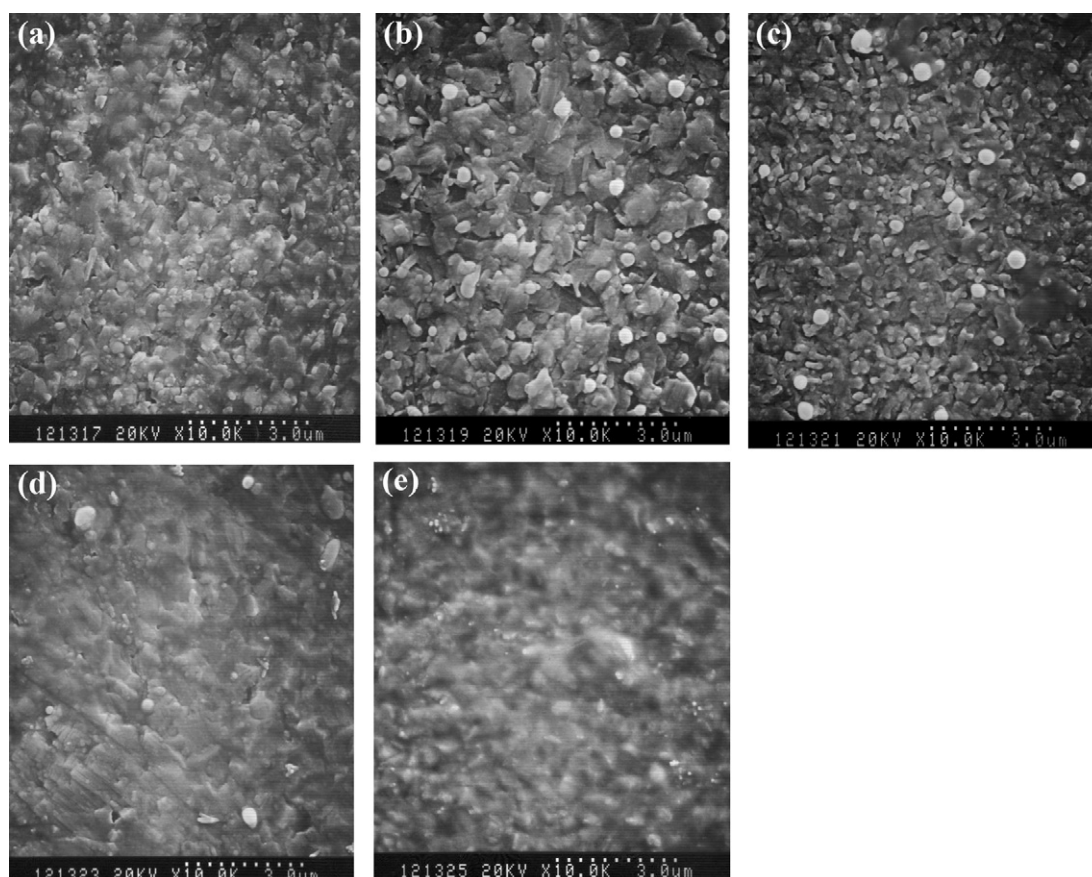


Fig. 1. SEM images of In_2Se_3 thin films deposited at substrate temperature varying from 350 to 500 °C. (a) IS350, (b) IS375, (c) IS400, (d) IS450 and (e) IS500.

Temperature dependent PL measurements were performed to characterize the luminescent property of the $\gamma\text{-In}_2\text{Se}_3$ films in temperature range of 10–300 K in a closed-cycle helium refrigerator system. A 532 nm solid state laser was used for Raman measurement in backscattering geometry. XRD spectra were taken under θ – 2θ scan employing $\text{Cu K}\alpha$ ($\lambda = 1.5405 \text{ \AA}$) radiation. For PL measurements, 532 nm (DPSS) continuous wave (CW) laser was used as an excitation light with excitation power fixed at 50 mW. The luminescent light was dispersed by a 0.5 m monochromator (Jobin Yvon triax 550) and detected by photomultiplier tube (Hamamatsu R928).

3. Results and discussion

The surface morphology of the films was examined in the SEM. Fig. 1 shows the top-view SEM images of the samples deposited at different temperatures. All the samples are consisted of horizontal lamellar structures with different grain sizes. At the lowest temperature (350 °C) the films deposited were demonstrated a small and rough morphology (Fig. 1(a)). As the temperature was increased, Fig. 1(b)–(d) confirms that the horizontal lamellar platelets of the films became larger and flatter. For example, as shown in Fig. 1(d), the surface of the IS450 films is homogeneous with individual and interconnected grains. The grains are closely packed and uniformly spread over the substrate without pinholes. As the substrate temperature again increased to 500 °C, the film morphology had changed from smooth lamellar structures to more rough crystallites (Fig. 1(e)). It was possible an indication of deteriorating revolution of the film quality with deposition temperature.

In order to clarify the crystal structure of the IS films, we characterized the IS films by XRD and Raman spectroscopy. Fig. 2 shows the θ – 2θ XRD spectra of IS films grown on $\text{Si}(111)$ substrate at different temperatures. All the samples exhibit narrow and strong peaks in the XRD patterns and all XRD pattern peaks were attributed to the diffractions of hexagonal $\gamma\text{-In}_2\text{Se}_3$. The

deposition temperature of the single-phase $\gamma\text{-In}_2\text{Se}_3$ film with a preferential growth orientation along $[0006]$ direction is 400 °C. In Fig. 3, we showed the room-temperature Raman spectra recorded in backscattering configuration from the IS films excited at 532 nm. There are four resolved phonon structures in each Raman spectrum, with one main mode located at 149.4 cm^{-1} . The two Raman modes located at 178.6 and 203.7 cm^{-1} have been observed in the reported Raman spectra of both $\gamma\text{-In}_2\text{Se}_3$ [16] or $\alpha\text{-In}_2\text{Se}_3$ [17,18]. On the other hand, the two Raman modes located at 149.4 and 227.6 cm^{-1} appears at the same wave numbers as in the reported

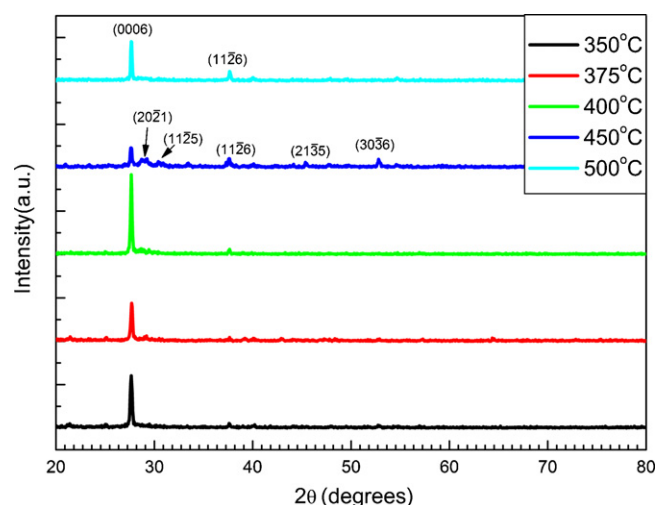


Fig. 2. X-ray diffraction patterns of In_2Se_3 thin films deposited at substrate temperature varying from 350 to 500 °C.

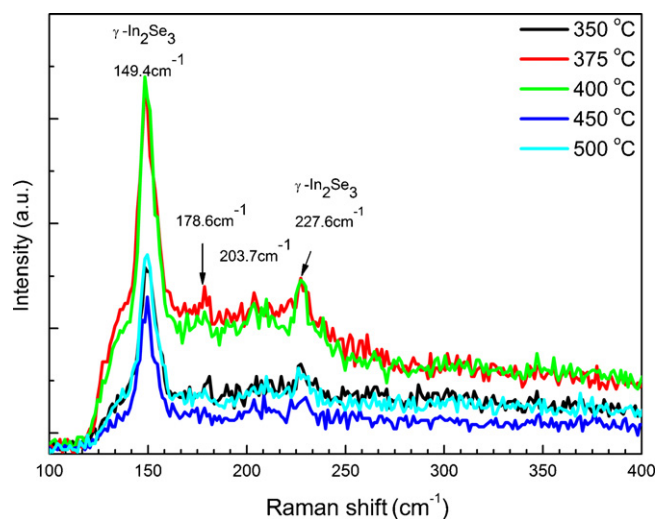


Fig. 3. Raman spectra of In_2Se_3 thin films deposited at substrate temperature varying from 350 to 500 °C.

Raman spectra of only the $\gamma\text{-In}_2\text{Se}_3$ [19,20]. Thus, the results of Raman scattering measurements indicate the IS sample studied here are the single-phase $\gamma\text{-In}_2\text{Se}_3$, which is consistent with the results of XRD diffraction measurements. Accordingly, single-phase $\gamma\text{-In}_2\text{Se}_3$ thin films were grown on (1 1 1) Si substrate at temperature at least as high as 350 °C.

Fig. 4 shows a series of PL spectra taken at room temperature (RT) using visible (532 nm) excitation. The samples deposited at different temperatures have the same PL spectra with a near band-edge (NBE) line located at 1.936, 1.944, 1.946, 1.948 and 1.948 eV for the IS350, IS375, IS400, IS450 and IS500 $\gamma\text{-In}_2\text{Se}_3$ samples, respectively. For PL spectra, the full width of the half maximum (FWHM) of the NBE line are 182, 96.5, 93.8, 87.3, and 89.4 meV, for the IS350, IS375, IS400, IS450 and IS500 $\gamma\text{-In}_2\text{Se}_3$ samples, respectively. The measured RT-NBE emissions at around 1.947 eV from the $\gamma\text{-In}_2\text{Se}_3$ films are reasonably consistent with the estimated values of previous reports, which were deduced from the low-temperature PL data by fitting to the Varshni's equation [13,14]. Our results thus indicate that epitaxial $\gamma\text{-In}_2\text{Se}_3$ films with strong RT-NBE emissions were grown by atmospheric MOCVD.

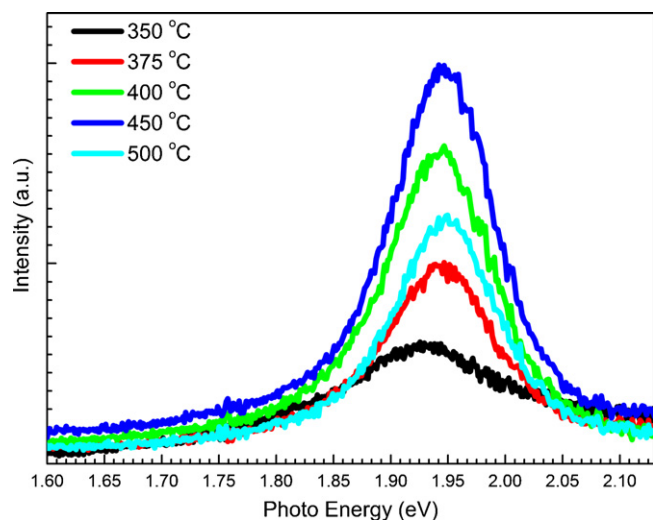


Fig. 4. Room-temperature PL spectra of $\gamma\text{-In}_2\text{Se}_3$ thin films deposited at substrate temperature varying from 350 to 500 °C.

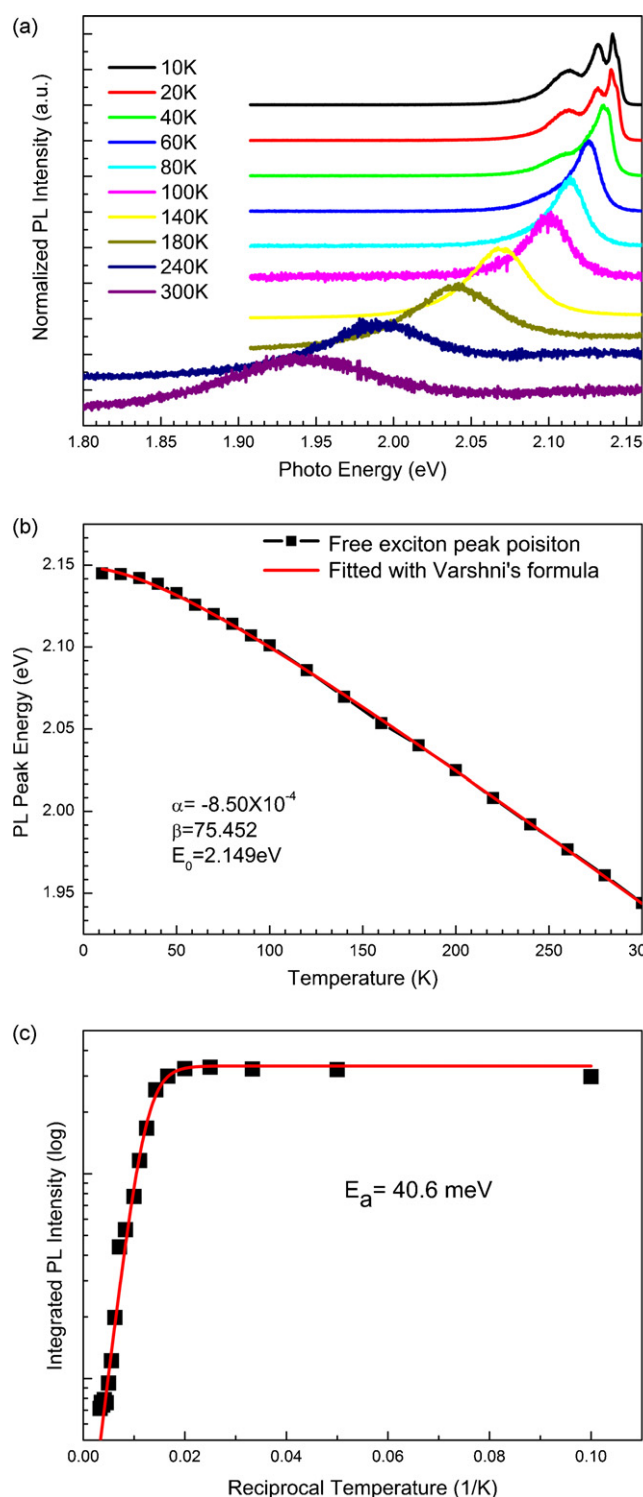


Fig. 5. (a) Temperature dependent PL spectra; (b) temperature dependence of PL peak energy; (c) the activation energy of free exciton emission of $\gamma\text{-In}_2\text{Se}_3$ film at grown temperature 450 °C. The solid line in (b) is the fitting curve according to Varshni equation.

In addition, the temperature evolution of PL spectra of IS450 sample with the strongest intensity and the narrowest FWHM of RT PL spectra was investigated as shown in Fig. 5(a). At 10 K, the emissions comprise three main peaks located at 2.141, 2.133 and 2.114 eV, as well as a shoulder at around 2.145 eV at the high energy side. It was found that the emission at 2.145 eV becomes eminent and finally dominant while the intensities of the other

three peaks decrease rapidly with increasing temperature. The three peaks located at 2.141, 2.133 and 2.114 eV became disappeared after the temperature was increased above 60 K. Therefore, the peak at 2.145 eV was attributed to free exciton emission and the other three peaks were attributed to bound excitons or defect-related emissions [13–15]. Fig. 5(b), the plot of PL peak energy versus temperature, shows a result of temperature-induced shrinkage and is well fitted by the Varshni empirical formula [21], $E_g(T) = E_g(0) + \alpha T^2 / (T + \beta)$, where $E_g(0)$ is the absolute zero value of the band gap, T is the temperature, $\alpha = dE_g/dT$ is the rate of change of the band gap with temperature, and β is physically associated with the Debye temperature. The fitting represented by the solid line in the figure revealed the fitting parameters of $E_g(0) = 2.149$ eV, $\alpha = -8.50 \times 10^{-4}$ eV/K, and $\beta = 75.5$ K. The measured PL peak energy redshifts by ~ 200 meV with increasing temperature from 10 to 300 K. Fig. 5(c) shows the integrated PL intensities of the free exciton emissions. In this figure, the solid squares represent the experimental results while the solid line represents a theoretical fit to the data with the thermal quenching expression: $I(T) = I_0 [1 + C \exp(-E_a/k_B T)]^{-1}$, where I_0 is the intensity at $T = 0$ K, C is a constant, E_a is an activation energy, and k_B is the Boltzmann constant. Indeed, the PL intensity increases almost exponentially with an activation energy from 10 to 300 K. This indicates that the PL originates from the recombination of the free excitons with a binding energy of about 41 meV. A large activation energy of the sample efficiently prevents carriers from thermal quenching and ensures strong emission up to room temperature. It explains the increase of the relative PL intensity of the γ -In₂Se₃ films with the increase of temperature. After the exciton is broken apart, electron is free to diffuse throughout the sample, and the PL is quenched. From our binding energy, 41 meV, we can estimate the exciton reduced mass of γ -In₂Se₃. With $\epsilon_r = 11.2$ [22,23], we get $\mu_{exc} = 0.38m_0$ for the isotropic value of the exciton reduced mass. This is fairly large and deserves for further studies on the physical properties of this highly anisotropic semiconductor [24,25].

4. Conclusion

In summary, good quality γ -In₂Se₃ films with room-temperature PL were successfully grown on Si(111) substrate using LT In_xSe_y buffer layer by atmospheric MOCVD. The crystal structure of the γ -In₂Se₃ films was determined by XRD and Raman spectroscopy. It was found that the films deposited at the temperature range of 350–500 °C are all single-phase γ -In₂Se₃ films. Raman scattering studies revealed one main mode located

at 149.4 cm⁻¹, the characteristic of the γ -In₂Se₃, which is absent in other In₂Se₃ phases. The temperature dependence of the near band-edge emission in the temperature region of 10–300 K has been investigated. At 10 K, the free exciton emissions was observed and located at 2.145 eV. At 300 K, a single PL peak showed that the band gap of γ -In₂Se₃ at room-temperature is about 1.947 eV. The measured peak energy of near band-edge emission redshifts by about 200 meV with increasing temperature from 10 to 300 K, and is expressed by, $E_g(T) = 2.149 + ((-8.50 \times 10^{-4})T^2 / (T + 75.5))$ eV. All these results can support that growth of high quality γ -In₂Se₃ films for a Cd-free buffer layer in solar cell formation will be possible.

Acknowledgment

This work was supported in part by the National Science Council under the Grant number NSC 95-2112-M-019-007-MY3.

References

- [1] M. Emziane, S. Marsillac, J.C. Bernède, Mater. Chem. Phys. 62 (2000) 84.
- [2] S. Popovic, B. Celustka, D. Bidjin, Phys. Status Solidi (A) 6 (1971) 699.
- [3] D. Bidjin, S. Popovic, B. Celustka, Phys. Status Solidi (A) 6 (1971) 295.
- [4] T. Ohtsuka, K. Nakanishi, T. Okamoto, A. Yamada, M. Konagai, U. Jahn, Jpn. J. Appl. Phys. Part 1 40 (2001) 509.
- [5] J. Jasinski, W. Swider, J. Washburn, Z. Liliental-Weber, A. Chaiken, K. Nauka, G.A. Gibson, C.C. Yang, Appl. Phys. Lett. 81 (2002) 4356.
- [6] G. Gordillo, C. Calderon, Sol. Energy Mater. Sol. Cells 77 (2003) 163.
- [7] J.P. Guesdon, B. Kobbi, C. Julien, M. Balkanski, Phys. Status Solidi (A) 102 (1987) 327.
- [8] S. Marsillac, J.C. Bernède, R. Le Ny, A. Conan, Vacuum 46 (1995) 1315.
- [9] T. Okamoto, A. Yamada, M. Konagai, J. Cryst. Growth 175/176 (1997) 1045.
- [10] T. Ohtsuka, T. Okamoto, A. Yamada, M. Konagai, J. Lumin. 87–89 (2000) 293.
- [11] H.J. Gysling, A.A. Wernberg, T.N. Blanton, Chem. Mater. 4 (1992) 900.
- [12] J. Cheon, J. Arnold, K.-M. Yu, E.D. Bourret, Chem. Mater. 7 (1995) 2273.
- [13] D.Y. Lyu, T.Y. Lin, J.H. Lin, S.C. Tseng, J.S. Hwang, H.P. Chiang, C.C. Chiang, S.M. Lan, Sol. Energy Mater. Sol. Cells 91 (2007) 888.
- [14] K.J. Chang, S.M. Lahn, J.Y. Chang, Appl. Phys. Lett. 89 (2006) 182118.
- [15] K.J. Chang, S.M. Lahn, Z.J. Xie, J.Y. Chang, W.Y. Uen, T.U. Lu, J.H. Lin, T.Y. Lin, J. Cryst. Growth 306 (2007) 283.
- [16] K. Kambas, C. Julien, M. Jouanne, A. Likforman, M. Guittard, Phys. Status Solidi (B) 124 (1984) K105.
- [17] R. Lewandowska, R. Bacewicz, J. Filipowicz, W. Paszkowicz, Mater. Res. Bull. 36 (2001) 2577.
- [18] K. Kambas, C. Julien, Mater. Res. Bull. 17 (1982) 1573.
- [19] S. Marsillac, A.M. Combat-Marie, J.C. Bernède, A. Conan, Thin Solid Films 288 (1996) 14.
- [20] I. Watanabe, T. Yamamoto, Jpn. J. Appl. Phys. 24 (1985) 1282.
- [21] Y.P. Varshni, Physica (Amsterdam) 34 (1967) 149.
- [22] C. Julien, M. Eddrief, M. Balkanski, A. Chevy, Phys. Rev. B 46 (1992) 2435.
- [23] C. Julien, A. Chlwy, D. Siapk, Phys. Status Solidi (A) 118 (1990) 553.
- [24] M.O. Godzaev, B.E. Sernelius, Phys. Rev. B 33 (1986) 8568.
- [25] Yu.P. Gnatenko, Yu.I. Zhirko, Phys. Status Solidi (A) 180 (1993) 147.